

Giant Collective Fluctuations of Charged Membranes at the Lamellar-to-Vesicle Unbinding Transition. 1. Characterization of a New Lipid Morphology by SANS, SAXS, and Electron Microscopy

Bruno Demé,[†] Monique Dubois,[‡] Thaddée Gulik-Krzywicki,[§] and Thomas Zemb^{*‡}

Institut Laue-Langevin, B.P. 156, F-38042 Grenoble Cedex 9, France, Service de Chimie Moléculaire, CEA Saclay, F-91191 Gif sur Yvette Cedex, France, and Centre de Génétique Moléculaire, CNRS, F-91190 Gif sur Yvette, France

Received May 15, 2001. In Final Form: September 3, 2001

We show the existence of a new and unexpected morphology of charged phospholipid membranes composed of pure dioleoylphosphatidylserine (DOPS, Na⁺) in the absence of added salt. This new morphology is characterized by giant collective fluctuations of locally lamellar stacks of membranes at the lamellar-to-vesicle unbinding transition. The DOPS dispersions have been studied in pure water and at rest using complementary techniques: small-angle scattering (neutron and X-ray) and freeze-fracture electron microscopy. In the present case of strong unscreened electrostatic interaction, we show that the order-to-disorder transition associated with the lamellar phase unbinding into vesicles is hidden by the presence of this intermediate state of strongly coupled undulating membranes where electrostatic and entropic forces compete. The giant collective fluctuations produce a texture analogous to that of an oyster shell as observed by freeze-fracture electron microscopy. Three microstructures are encountered along the dilution line of bulk samples: an L_α lamellar phase with linear swelling, the lamellar oyster shell state characterized by giant collective fluctuations, and finally stable single- or multilayer vesicles formed spontaneously by a peeling mechanism of the fluctuating membranes as suggested by the period of the undulations close to the size of the vesicles.

Introduction

Binary phase diagrams of phospholipids show the typical sequence of phases upon dilution: L_β, L_α, followed by thermodynamically stable vesicles.^{1,2} This is true for most phospholipids, but the mechanism by which an ordered lamellar phase transforms into vesicles, the so-called *unbinding transition*, is still questioned. We examine here the phase behavior of dioleoylphosphatidylserine (DOPS, Na⁺), a model anionic phospholipid with molten chains at room temperature ($T_{\text{gel/fluid}} = -11$ °C in excess water) and bearing one net negative charge per headgroup at neutral pH.

There exists to our knowledge no data reporting values of a maximum swelling of lipids from the phosphatidylserine series in pure water. The equation of state, binding together in a formal manner the temperature, the osmotic pressure, and the concentration (or periodicity), is not known for any lipid of this family. From the 700 papers on phosphatidylserines reported in the database LIPIDAT,³ none of them gives an indication of a maximum swelling in the absence of salt (or buffer) and only two studies report explicitly on the binary phase diagram of phosphatidylserine^{4,5} in these conditions.

In pure water, with only counterions present (no added salt), one expects a strong dominating electrostatic contribution and a high swelling limit before the transition to vesicles where repulsive interactions between membranes vanish. Depending on whether membranes are stiff or flexible, an additional entropic repulsive contribution may come into play, accounting for out-of-plane fluctuations. In the regime of strongly fluctuating membranes (deviations from the midplane are much greater than lamellar periodicity), additivity of molecular interactions and entropic forces is no longer valid and renormalization theories need to be considered. However, these have up to now only given trends in comparison to the simple case of stiff membranes where only additive molecular interactions need to be taken into account (hydration, van der Waals, electrostatics). In such systems, the periodicity d is related to the volume fraction ϕ and to the bilayer thickness $2t$ by an "ideal swelling" relation: $d = 2t\phi^{-1}$. A logarithmic correction has been proposed to account for small fluctuations but has been questioned due to mathematical inconsistency in the derivation in the case of smectics⁶ and sponge phases.⁷ The nonlinearity of swelling when electrostatics competes with undulations has been considered recently by von Berlepsch and de Vries⁸ in the case of weakly charged bilayers.

For the only other known case where a highly swollen lamellar phase competes with spontaneous vesiculation, a linear relation between the maximum swelling and the Debye screening length has been observed.⁹ This linear relation is set by the equality of the osmotic pressure in

* To whom correspondence should be addressed. E-mail: zemb@drecam.saclay.cea.fr.

[†] Institut Laue-Langevin.

[‡] Service de Chimie Moléculaire, CEA Saclay.

[§] Centre de Génétique Moléculaire, CNRS.

(1) Seddon, J. M.; Templer, R. H. In *Structures and Dynamics of Membranes*; Lipowski, R., Sackmann, E., Eds.; Elsevier: Amsterdam, 1995; Vol. 1, pp 97–160.

(2) Dubois, M.; Zemb, Th. *Curr. Opin. Colloid Interface Sci.* **2000**, *5*, 27–37.

(3) Cevc, G.; Watts, A.; Marsh, D. *Biochemistry* **1981**, *20*, 4955–4965.

(4) Hauser, H.; Shipley, G. G. *Biochemistry* **1983**, *22*, 2171–2178.

(5) Dubois, M.; Zemb, Th.; Fuller, N.; Rand, R. P.; Parsegian, V. A. *J. Chem. Phys.* **1998**, *108*, 7855–7869.

(6) Helfrich, W. *Eur. Phys. J.* **1998**, *B1*, 481–489.

(7) Daicic, J.; Olsson, U.; Wennerstroem, H.; Jerke, G.; Schurtenberger, P. *Phys. Rev. E* **1997**, *56*, 1278–1279.

(8) von Berlepsch, H.; de Vries, R. *Eur. Phys. J. E* **2000**, *1*, 141–152.

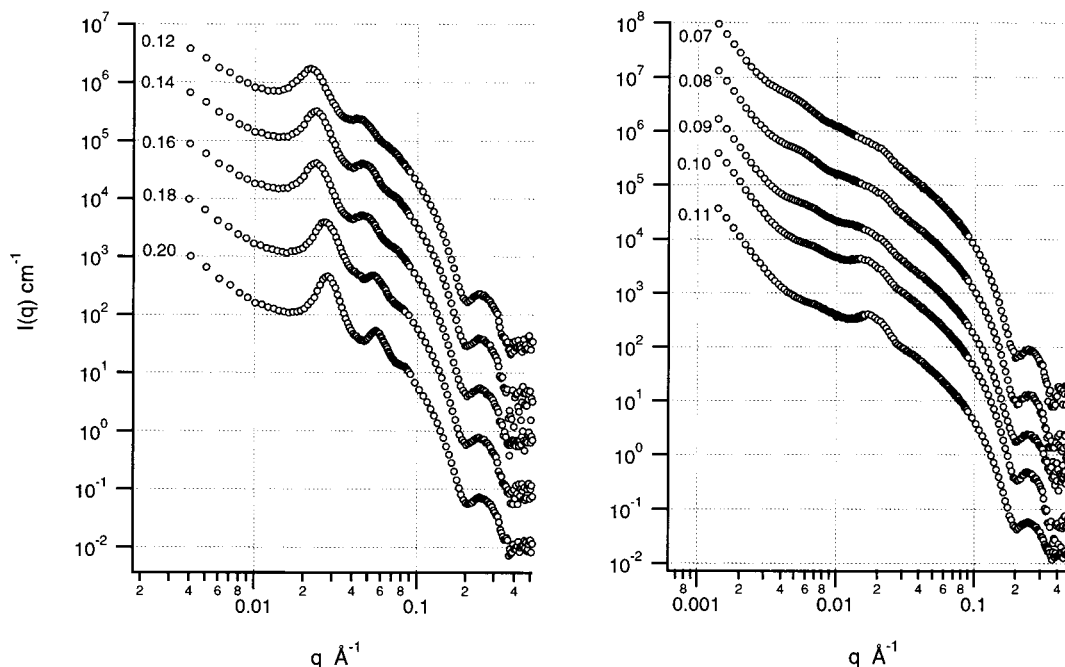


Figure 1. Dilution experiment of DOPS bulk samples at room temperature (25 °C) followed by SANS. Left: stiff electrostatic phase, from bottom to top $\phi = 0.20$ – 0.12 (w/w). Right: soft lamellar phase in the oyster shell state, from bottom to top $\phi = 0.11$ – 0.07 (w/w). $I(q)$ in cm^{-1} for the left and right lower curves; other curves are offset for clarity.

the smectic and vesicle phases, the equivalent of an Onsager transition, but for rigid bilayers.¹⁰ One of our aims is to investigate if this is still true in pure water, that is, when there is no added salt or electrolyte background such as dissociated monomers (low critical micelle concentration). In this case, the repulsive pressure is known as the Langmuir equation:¹¹

$$\Pi(d_w) = \frac{\pi k T}{2L_b} \frac{1}{d_w^2} \quad (1)$$

where L_b is the Bjerrum length (7.2 Å in water at room temperature) and d_w is the water layer thickness ($d_w = d - 2\delta$). This expression does not depend on values of the elastic bending constants.

In the case of pure solutions of the anionic phospholipid DOPS, we would like to address the following questions: (1) What is the swelling law of a soft lamellar structure in unscreened electrostatic repulsion? (2) Are fluctuations in the range of interlayer separation distances important? (3) Are there correlated undulations of neighboring membranes? To this aim, we used small-angle scattering (neutron and X-ray) and freeze-fracture electron microscopy.

The experimental results presented here are the first part of a study aimed at giving a complete description of the structures and thermodynamics of the observed phases in well-defined regimes and at the transition between these regimes in the strong unscreened electrostatic interaction case. The measurements described in these two papers make it possible for theoreticians to think quantitatively about the dramatic effect of fluctuations in a charged lamellar system. For example, it was predicted by de Vries that highly charged membranes could have a compress-

ibility and hence osmotic pressures influenced by the presence of undulations.¹² In the case of weakly charged bilayers, the presence of undulations far from a macroscopic solid interface has been evidenced recently by Salamat et al.¹³

The equation of state derived from scattering experiments under controlled osmotic pressure via equilibration with polymer solutions or vapor pressure is described in the second part of the present paper.¹⁴

Materials and Methods

DOPS (1,2-dioleoyl-*sn*-glycero-3-phospho-L-serine, sodium salt, MW = 810) was purchased from Avanti Polar Lipids (Alabaster, AL) and was dialyzed versus Milli-Q water (Millipore, Bedford, MA) to ensure elimination of residual salt. Thin-layer chromatography showed a single spot corresponding to DOPS and no detectable organic impurity. The pH of DOPS samples was around 9, and conductivity after equilibration and several replacements of the water in the reservoir was of the order of 10 μSi .

Small-angle neutron scattering (SANS) experiments were performed on D22¹⁵ at the Institut Laue-Langevin, Grenoble, France. Small-angle X-ray scattering (SAXS) experiments were performed on a home-built camera in pinhole geometry.¹⁶

Freeze-fracture electron microscopy (EM) was performed on samples prepared in a H₂O/glycerol mixture (70/30 v/v), using the protocol previously described.¹⁷

Results

Figure 1 shows SANS curves obtained for a series of volume fractions of DOPS in D₂O ranging from 0.20 to 0.07. Important features come out from these scattering curves measured to our knowledge for the first time over

(12) de Vries, R. *Phys. Rev. E* **1997**, *56*, 1879–1886.

(13) Salamat, G.; de Vries, R.; Kaler, E. W.; Satija, S.; Sung, L. P. *Langmuir* **2000**, *16*, 102–107.

(14) Demé, B.; Dubois, M.; Zemb, Th. *Langmuir* **2001**, *17*, 1005–1013.

(15) <http://www.ill.fr/YellowBook/D22/>.

(16) Le Flanchec, V.; Gazeau, D.; Taboury, J.; Zemb, Th. *J. Appl. Crystallogr.* **1996**, *29*, 110–117.

(17) Gulik-Krzywicki, Th. *Curr. Opin. Colloid Interface Sci.* **1997**, *2*, 137–144.

(9) Dubois, M.; Zemb, Th.; Belloni, L.; Delville, A.; Levitz, P.; Setton, R. *J. Chem. Phys.* **1992**, *96* (3), 2278–2286.

(10) Zemb, Th.; Belloni, L.; Dubois, M.; Marcelja, S. *Prog. Colloid Polym. Sci.* **1992**, *89*, 33–38.

(11) Israelachvili, J. N. *Intermolecular and surface forces*, 2nd ed.; Academic Press: San Diego, CA, 1992.

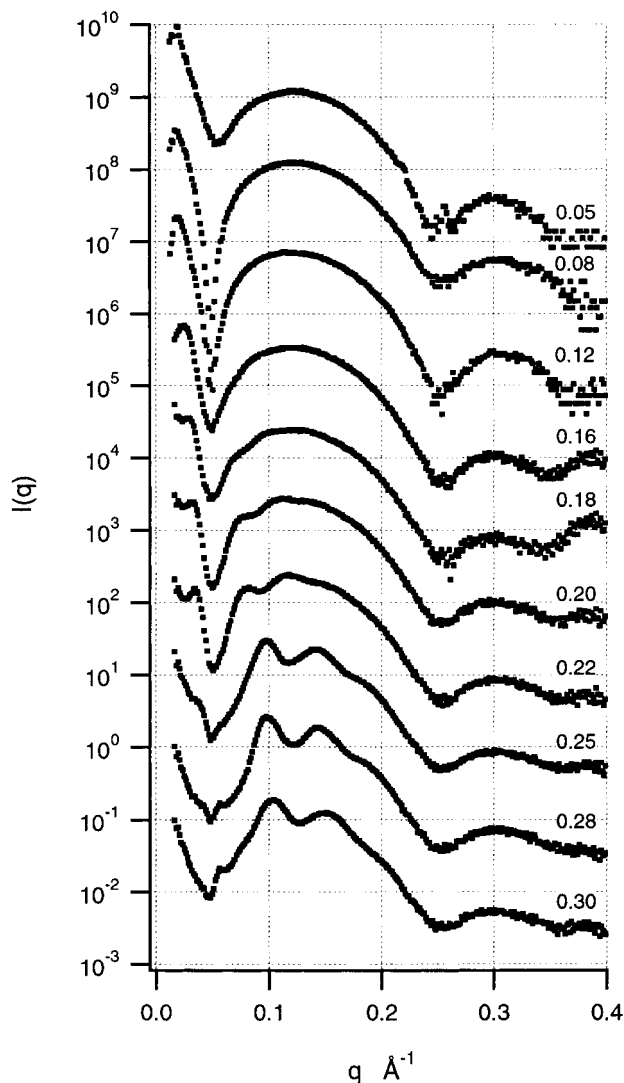


Figure 2. Dilution experiment of DOPS bulk samples at room temperature (25 °C) followed by SAXS. From bottom to top: $\phi = 0.30$ – 0.05 (w/w). $I(q)$ in cm^{-1} for the lower curve at $\phi = 0.30$; other curves are offset for clarity.

nearly three decades in q and six decades in intensity for the more dilute samples. The minima of the membrane form factor are observed at high q , while several peaks corresponding to the lamellar structure factor are visible at low q . The first and second minima of the membrane form factor are located at $q = 0.20$ and 0.38 \AA^{-1} . From the position of the first minimum, the thickness of the layer of aliphatic chains can be estimated since the chain–head contrast is the dominating term. We find here a thickness $2t = 31 \text{ \AA}$. A detailed density profile including the headgroup contribution will be used for the X-ray form factor where the head–solvent contrast term dominates. The structure factor of dilute samples is observed at low q in a range of scattering vectors where it is only modulated by the q^{-2} decay of the membrane form factor. Three quasi-Bragg peaks are visible for volume fractions $\phi > 0.14$, but only one broad (smectic?) order is still visible below $\phi = 0.10$.

Figure 2 shows the scattering produced by DOPS dispersions in water using SAXS in pinhole geometry. Again, the scattering curves contain information both on the bilayer structure and on membrane interactions. In dilute samples where the structure factor disappears toward low q , the membrane form factor can be fitted

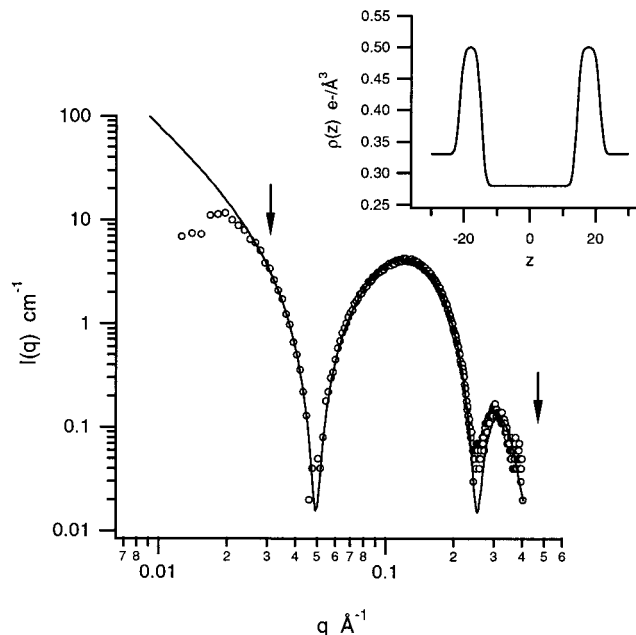


Figure 3. SAXS of a dilute DOPS sample ($\phi = 0.065$ w/w, $S(q) \sim 1$). The solid line is a fit to the data (fitting interval between arrows) using a three-level electron density profile (inset).

using a three-level electron density profile accounting for the chains, the heads, and the solvent.¹⁸ The best fit obtained for a dilute sample at $\phi = 0.065$ is shown in Figure 3 with the corresponding electron density profile in the inset. The arrows indicate the q -range considered to fit the data. The fit (including 5 free parameters) yields an electron density of $0.28 \text{ e}^{-}/\text{\AA}^3$ for aliphatic chains, $0.50 \text{ e}^{-}/\text{\AA}^3$ for the layer of hydrated headgroups, $28.6 \pm 0.3 \text{ \AA}$ and $43.9 \pm 0.3 \text{ \AA}$ for the apolar and total membrane thicknesses, respectively, and a roughness of 4 \AA . Thicknesses and densities determined here are completely independent from swelling (or concentration) and do not depend on the small-angle scattering, since the membrane form factor is well separated from the low- q region. The direct membrane thickness determination avoids problems inherent to other methods, like for instance when the bilayer thickness is derived from the linear relation between the smectic periodicity and $1/\phi$. This relation is only valid in the absence of fluctuations¹⁹ or defect regions containing excess water.²⁰ Another indirect method is based on the reconstruction of Bragg peak amplitudes modulated by the form factor.²¹

We have derived the structure factors of the membrane stacks for the different concentrations studied. The result is a series of normalized X-ray structure factors $S(q)$ for the stack of charged membranes shown in Figure 4A. Four Bragg orders can be seen for the L_{α} phase at a volume fraction of 0.30. Using the parameters obtained from the fit to the X-ray data, we have calculated the neutron form factor and extracted $S(q)$ from the neutron data shown in Figure 1. These are shown in Figure 4B. At concentrations below 0.1, the samples are still dispersions of strongly repulsive bilayers. Thus, their smectic nature can hardly

(18) Cantù, L.; Corti, M.; Del Favero, E.; Dubois, M.; Zemb, Th. *J. Phys. Chem. B* **1998**, *102*, 5737–5743.

(19) Nagle, J. F. In *Phase Transitions in Complex Fluids*; Toledano, P., Figueiredo, N., Eds.; World Scientific: Singapore, 1998; pp 247–269.

(20) Nagle, J. F.; Tristram-Nagle, S. *Biochim. Biophys. Acta* **2000**, *1469*, 159–195.

(21) Petrache, H. I.; Tristram-Nagle, S.; Nagle, J. F. *Chem. Phys. Lipids* **1998**, *95*, 83–94.

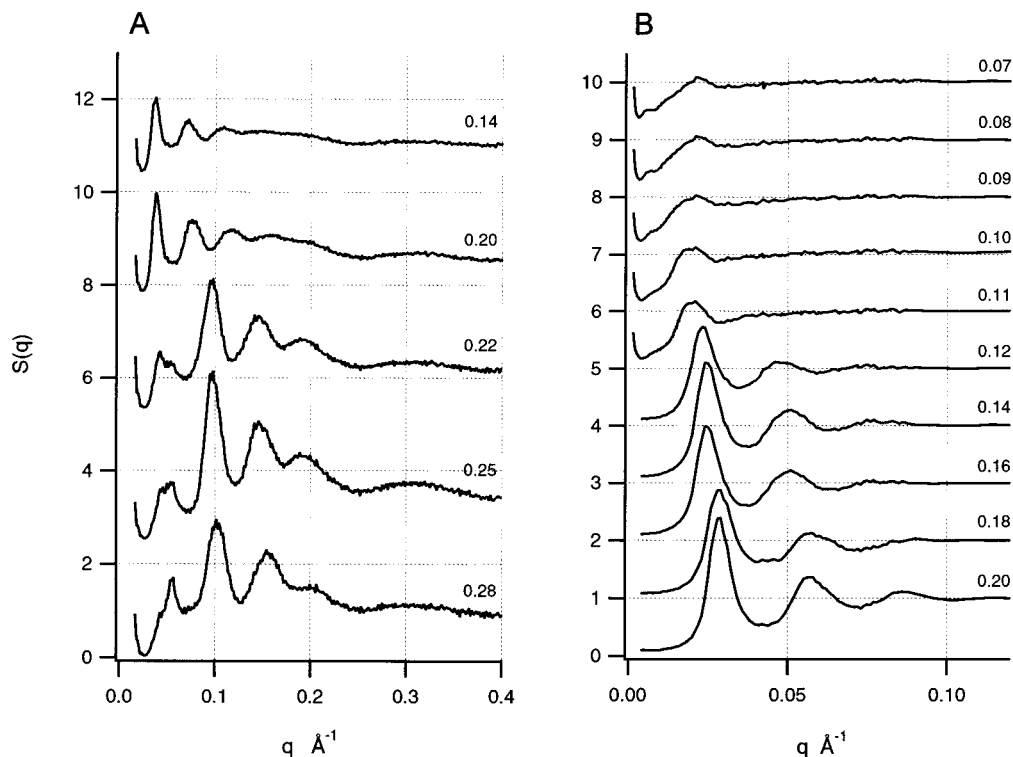


Figure 4. (A) X-ray experimental structure factors $S(q)$ obtained by dividing $I(q)$ by the experimental form factor. From bottom to top: $\phi = 0.28$ – 0.14 . (B) Neutron structure factors $S(q)$ obtained by dividing $I(q)$ by the neutron form factor calculated with parameters obtained from the fit to the X-ray data (chain and head thicknesses, densities, hydration, roughness). Bottom to top: $\phi = 0.20$ – 0.07 . The series of neutron and X-ray $S(q)$ evidences the fast disappearance of quasi-Bragg peaks while the smectic layering is still present. Lower curves are to the scale ($\lim_{q \rightarrow \infty} S(q) = 1$); other curves are offset for clarity.

be questioned. In the absence of added salt, the ionic strength is of the order of 10^{-5} (pH ~ 9), and the Debye screening length (100 nm) is of the order of the stack periodicity. Therefore, it is obvious that strong repulsions between highly charged bilayers are still present.

In Figure 5, we have reported the swelling versus $1/\phi$ by regrouping results obtained by SANS, SAXS, and freeze-fracture electron microscopy. For periodicities below 250 Å, the swelling is linear, but above this value it deviates from linearity. A fit to the data in the linear regime gives a bilayer thickness of 42.2 Å, consistent with the value derived from the experimental X-ray membrane form factor (43.9 Å). At higher dilution, deviation from linearity has already been observed in the case of a cationic synthetic lipid and with DMPC membranes decorated by soluble polymer chains.²² But in this latter case, periodicities were above those expected for a linear swelling and were explained in terms of excess area required to build a lamellar structure with strongly bent membranes. Fluctuations leading to a nonlinear swelling are common to uncharged membranes.²³ However, fluctuations lead to an additional repulsive contribution in the force balance²⁴ and enhance the swelling, that is, relation 1 becomes $d > 2t/\Phi$. Here, we have a negative deviation from linearity, that is, $d < 2t/\Phi$. This means that correlated undulations which can be seen on the electron micrographs of Figure 6 have a direct consequence: the coexistence of defects inducing the presence of regions with more water than in strongly undulating bilayer stacks. The simplest case of defect is at the contact point between large (> 1

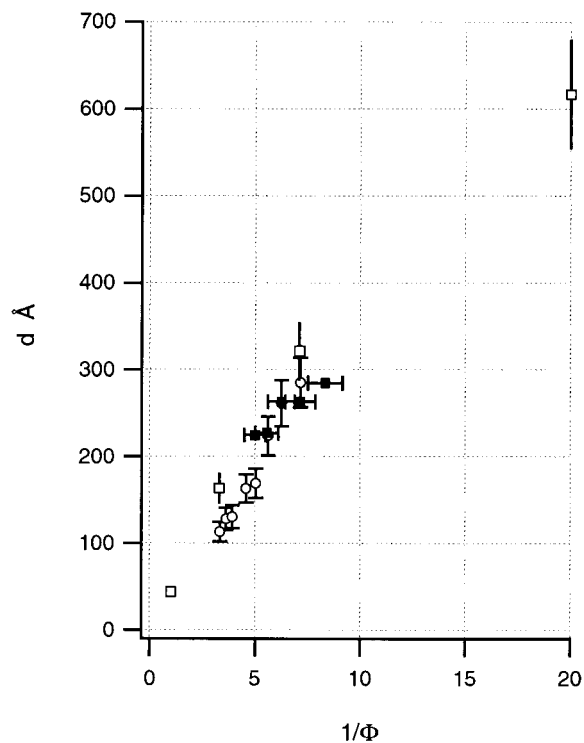


Figure 5. Plot of the lamellar periodicity vs $1/\phi$ as obtained by SANS, SAXS, and microscopy, showing the nonlinear behavior above 250 Å.

(22) Demé, B.; Dubois, M.; Zemb, Th.; Cabane, B. *J. Phys. Chem.* **1996**, *100*, 3828–3838; *Colloids Surf. A* **1997**, *121*, 135–143.

(23) Dubois, M.; Zemb, Th. *Langmuir* **1991**, *7*, 1352–1360.

(24) Helfrich, W. In *Phase Transition in Soft Condensed Matter*; NATO ASI Ser. B; Plenum Press: New York, 1989; Vol. 211, pp 271–281.

μm) multilayer anion-type lamellar crystallites.²⁰ Between spherical multilayers in contact, excess water is needed to fill space. This behavior induces a nonlinear swelling with $d < 2t/\Phi$. In the case of cationic bilayers, in the

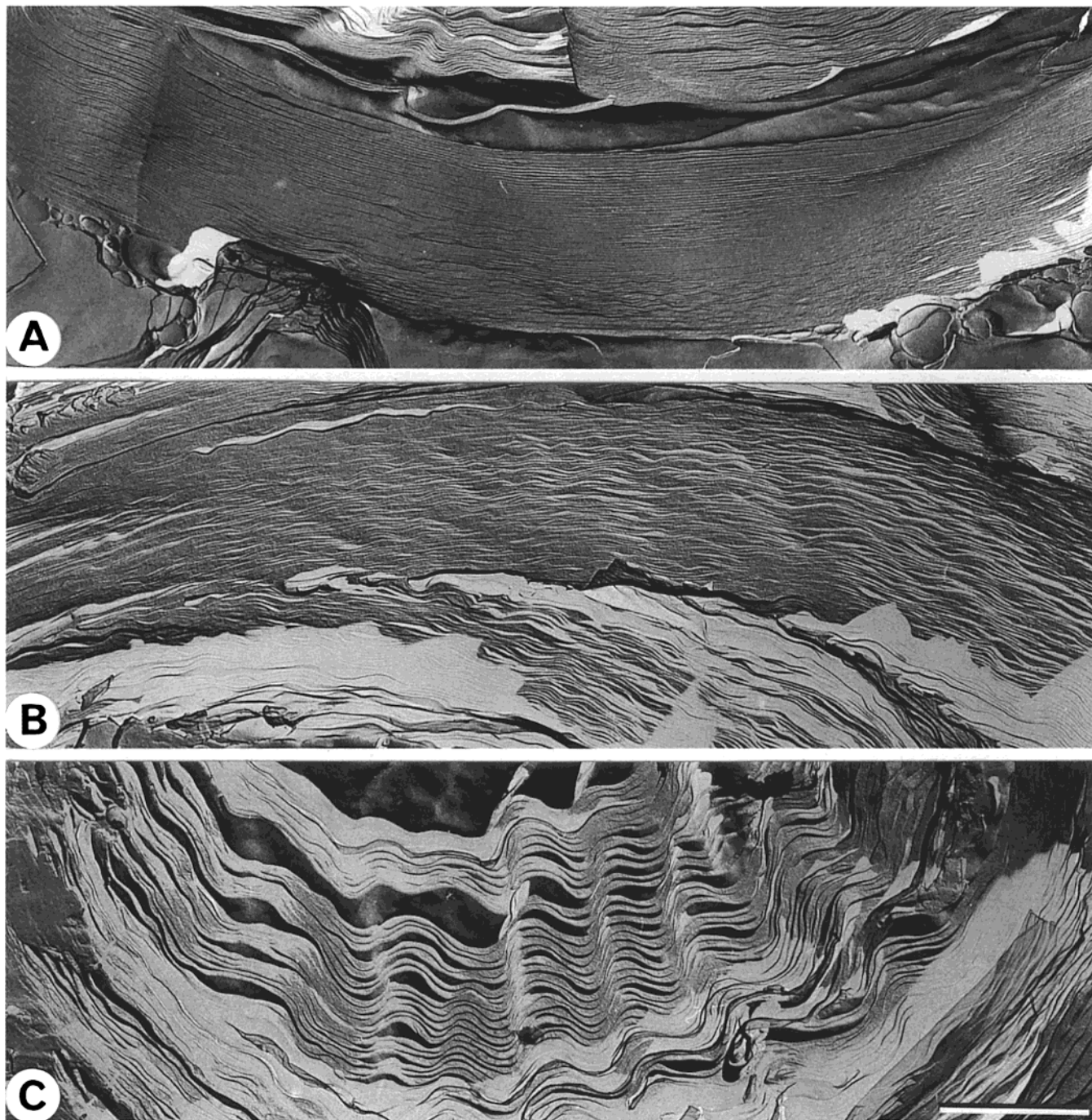


Figure 6. Freeze-fracture electron microscopy of DOPS samples: (A) regular lamellar phase ($\phi = 0.30$), (B) lamellar phase with low-amplitude uncorrelated fluctuations ($\phi = 0.14$), and (C) giant correlated fluctuations in a stack of membranes ($\phi = 0.05$). The bar represents 1 μm .

absence of salt too, long-range ordering of defects has been shown to be the origin of colored iridescence of samples.²³

In the case of DOPS reported here, the nonlinear swelling is not only due to steric interactions. Giant undulations appear on the images shown in Figure 6, where samples at volume fractions $\phi = 0.30$, 0.14, and 0.05 are compared at the same magnification. The crucial point is the strong increase of fluctuations seen upon dilution and the evolution from noncorrelated to correlated fluctuations. At $\phi = 0.05$, the range over which fluctuations are correlated corresponds to stacks of several membranes and the typical wavelength associated with these fluctuations is of the order of 5 times the periodicity. The fluctuations are different from the egg-carton structure

proposed by Klösgen & Helfrich and Antonietti & Thunemann,²⁵ which relies on correlated perpendicular surface waves producing the egg-carton structure. In the case of DOPS, the one-dimensional nature of the dominating undulations is evidenced in regions of the micrographs where the fracture plane is not perpendicular to the layers. In these regions, the texture is an analogue to that of an oyster shell.

Further dilution without input of energy or shearing of the sample produces a dispersion of vesicles. A typical

(25) Klösgen, B.; Helfrich, W. *Eur. Biophys. J.* **1993**, *22*, 329–340. Antonietti, M.; Thunemann, A. *Curr. Opin. Colloid Interface Sci.* **1996**, *1*, 667–671.

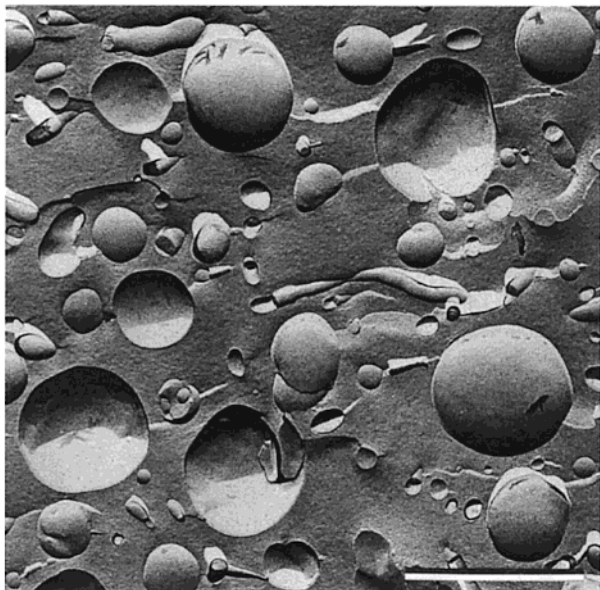


Figure 7. Spontaneous vesicles as seen in dilute samples by freeze-fracture electron microscopy. The bar represents 1 μm .

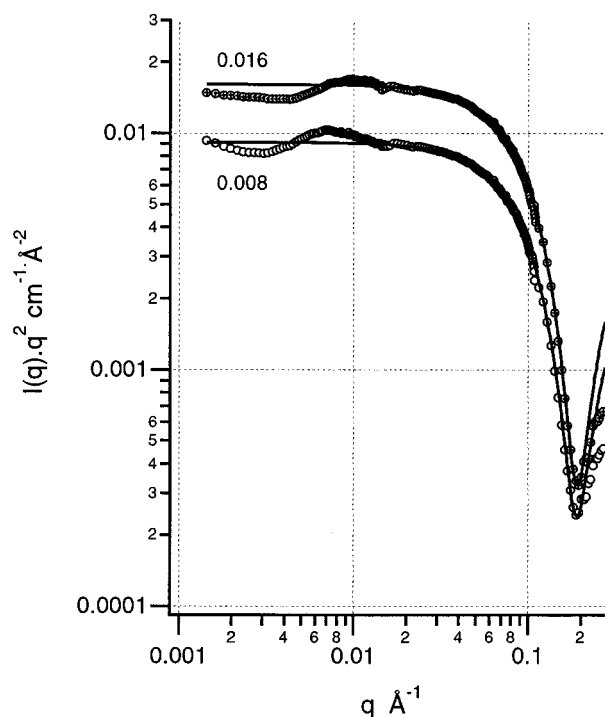


Figure 8. SANS curves ($\log[I(q) q^2]$ vs $\log(q)$) plot) observed in dilute samples prepared at $\phi = 0.016$ and 0.008 , where only vesicles are present. The solid lines are fits to the data in absolute scale using a single layer form factor. Given a fixed scattering length density contrast ($6.36 \times 10^{-6} \text{ \AA}^{-2}$), the fitted volume fractions are 0.0165 and 0.0094 , respectively, in excellent agreement with the preparation data. Note the remaining soft peak at low q resulting from the mean membrane–membrane distance of adjacent vesicles.

image obtained by freeze-fracture electron microscopy is shown in Figure 7. The corresponding SANS is shown in Figure 8. The curves show a nearly pure form factor of bilayers and a small oscillation due to the mean distance between membranes of adjacent vesicles or to residual oligolamellar vesicles producing a broad smectic correlation peak. The peak position corresponds to 600 and 900 \AA at volume fractions of 0.016 and 0.008 , respectively. Microscopy confirms that a polydisperse dispersion of

vesicles with diameters in the range of 500 – 5000 \AA is produced (Figure 7). These dispersions of spontaneous vesicles are stable upon time and after heating/cooling cycles and are therefore supposed to correspond to thermodynamic stability. This is expected from the general theory of two-component vesicles²⁶ and observed here for one-component vesicles as explained further on in the discussion.

Discussion

The driving force for this undulation may be found in surface charge fluctuations²⁷ or in the correlation of large fluctuations due to a local coupling mechanism analogue to an Onsager transition. Compared to random fluctuations, correlated fluctuations of adjacent bilayers increase the available volume for dissociated counterions. We know that in the absence of salt the osmotic pressure is dominated by the counterion contribution. Correlating fluctuations is a way to avoid locally concentrated counterions, a phenomenon leading to the formation of “bottlenecks” that would occur if fluctuations were uncorrelated.

There are two possible mechanisms for formation of stable vesicles in a binary solution of charged bilayers:

(I) The symmetry is broken by an inside/outside ionic strength difference. For typical vesicle radii in the range of 500 – 5000 \AA and with monovalent counterions, electroneutrality of the inside volume requires an average inside concentration to be of the order of 0.1 M , while the outside concentration of counterions vanishes. This asymmetry is at the origin of the nonlinearity of refractive indexes measured for other stable spontaneous vesicles obtained in the absence of salt.²⁸ Since area per headgroup is ionic strength dependent, an asymmetry of a few percent of the area per molecule inside or outside is enough to induce an instability of the membrane and formation of vesicles with a diameter of the order of 100 times the molecular length.

(II) Another mechanism is intrinsic to Poisson–Boltzmann electrostatics of charged bilayers. At high dilution, the bending constant associated with Gaussian curvature is highly negative^{29,30} which means that formation of closed objects is favored by intrinsic properties of highly charged membranes in the absence of salt.^{31,32}

Back to the intermediate state of the membranes which appear on the pictures with a shape characteristic of an oyster shell, we can extract the in-plane persistence length of the membranes and the typical length scale of the out-of-plane fluctuations. Plotting the SANS data in the coordinates used for locally flat aggregates ($\log[I(q) q^2]$ vs $\log(q)$) shows a peculiar feature: the growing of a very large scale superstructure peak (Figure 9). If we associate a typical length scale s to this superstructure peak with $s = 2\pi/q_s$, we find $s \approx 4d$ in the range of existence of the oyster shell state.

The broadening of the quasi-Bragg peaks together with the appearance of a superstructure peak (s) and correlated

(26) Jung, H. T.; Coldren, B.; Zasadzinski, J. A.; Iampietro, D. J.; Kaler, E. W. *Proc. Natl. Acad. Sci. U.S.A.* **2001**, *98*, 1353–1357.

(27) R. R. Netz proposes that strong surface density fluctuations of partly bound counterions are at the origin of the strong fluctuations apparent in the oyster shell state.

(28) Radlinska, E. Z.; Ninham, B. W.; Dalbiez, J. P.; Zemb, Th. *Colloids Surf.* **1990**, *46*, 213–230.

(29) Fogden, A.; Daicic, J.; Ninham, B. W. *Physica A* **1996**, *234*, 167–188.

(30) Fogden, A.; Daicic, J. *Colloids Surf., A* **1997**, *129/130*, 157–165.

(31) Fogden, A.; Ninham, B. W. *Adv. Colloid Interface Sci.* **1999**, *83*, 85–110.

(32) Fogden, A.; Daicic, J.; Kidane, A. *J. Phys. II* **1997**, *7*, 229–248.

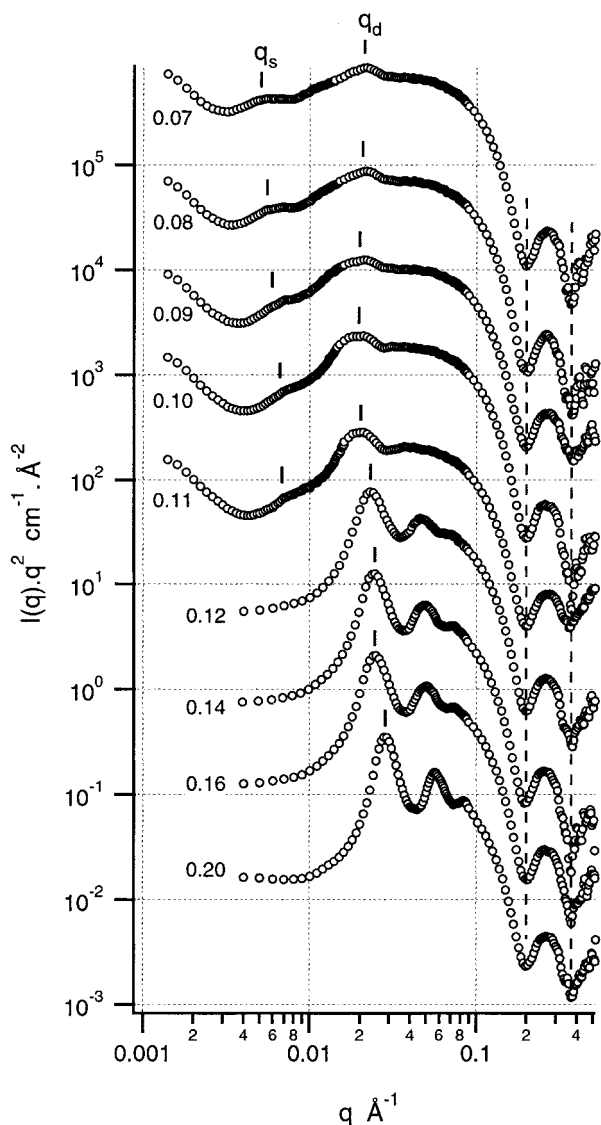


Figure 9. SANS curves ($\log[I(q)q^2]$ vs $\log(q)$) plot) obtained for different volume fractions (from bottom to top, $\phi = 0.20$ – 0.07). The oyster shell state corresponds to volume fractions below 11%, with the soft superstructure peak appearing at low q (S). $I(q)$ in $\text{cm}^{-1} \text{Å}^{-2}$ for the lower curve; other curves are offset for clarity.

fluctuations with the same length scale strongly supports that one-dimensional large amplitude undulations affect stacks of parallel membranes until formation of the oyster shell state (Figure 10). In the pure oyster shell regime shown in Figure 6 and at the volume fraction $\Phi = 0.05$, we observe an average fluctuation $\langle u \rangle$ around the mean position of a given bilayer, typically 4–6 times the period d . A larger number of layers, of the order of 10–30, appear in stacks of correlated membranes on the pictures. The stack is correlated in a direction perpendicular to the bilayers on a length ξ_{\perp} which is therefore 10–30 times the periodicity. Considering undulations of a given bilayer, the micrographs suggest an in-plane persistence length ξ_{\parallel} typically 4–6 times the periodicity d and identified to the in-plane periodicity s at the origin of the peak appearing at low q at $s = 2\xi_{\parallel}$. Lipowsky and Leibler³³ have considered the case where a strong exponential repulsive force and a dispersion force combine. They have identified theoretically a strong fluctuation regime which

(33) Lipowsky, R.; Leibler, S. *Phys. Rev. Lett.* **1986**, *56*, 2541–2544.

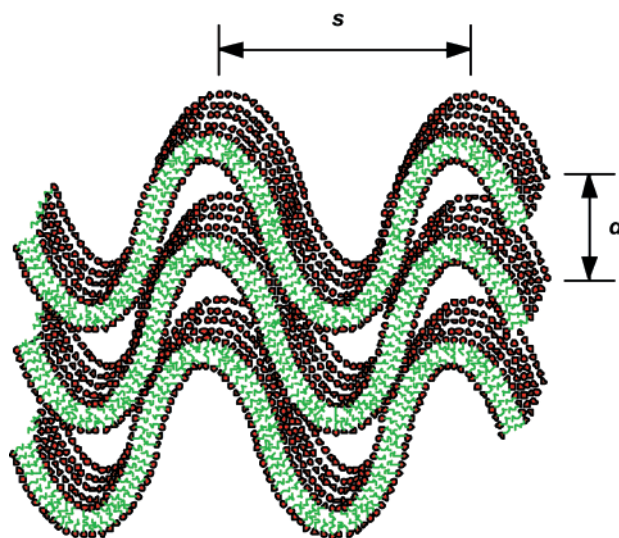


Figure 10. Sketch of the oyster shell microstructure. The maximum smectic periodicity d detected is of the order of 700 Å, at which unbinding occurs. In the intermediate oyster shell state, a superstructure s is detected on scattering patterns.

gives the following relation between perpendicular and parallel (in-plane) correlation lengths:

$$\xi_{\perp} = (kT/\kappa)^{1/2} \xi_{\parallel} \approx 0.3 \xi_{\parallel} \quad (2)$$

If we take numerical values of the bending constant out of the table published by Daicic⁷, we conclude that ξ_{\perp} should be less than d . And if we try now to identify these quantities in the oyster shell state, we find that the in-plane correlation length gives rise to the superstructure peak $s = 2\xi_{\parallel} \approx 5d \approx \xi_{\perp}/4$ and hence $\xi_{\parallel} \approx \xi_{\perp}/8$, a result consistent with the theoretical prediction. Other evaluations estimate maximum periodicity and in-plane correlation length to be approximately equal, $\xi_{\parallel} \approx d$.^{34,35} Our experimental result ($s \sim 4d$) is thus in qualitative agreement with theoretical expectations.

Conclusion

Using simple dilution and structural characterization of DOPS dispersions, we have encountered four distinct states:

(1) An L_{α} lamellar phase made of regularly spaced and flat bilayers in strong electrostatic repulsion, where no detectable fluctuations can be triggered by thermal energy at room temperature. This lamellar phase is present under the form of large multilayer polydisperse onion-type aggregates ($\phi > 0.30$).

(2) An L_{α} lamellar phase with low-amplitude ($u < d$) uncorrelated fluctuations ($\phi = 0.14$).

(3) The oyster shell state, characterized by giant ($u > d$) collective undulations of the membranes, vanishing broad quasi-Bragg peaks, and an in-plane persistence length equal to 4–6 times the smectic periodicity ($0.11 > \phi > 0.05$).

(4) Spontaneous stable vesicles, observed both by EM and SANS ($\phi < 0.05$). These vesicles are of the size of the spontaneous small unilamellar vesicles discovered by Talmon et al. in cationic double-chain surfactants in the absence of salt.³⁶

(34) Morse, D. C. *Phys. Rev. E* **1994**, *50*, 2423–2426.

(35) Morse, D. C.; Milner, S. T. *Phys. Rev. E* **1995**, *52*, 5918–5945.

(36) Talmon, Y.; Evans, D. F.; Ninham, B. W. *Science* **1983**, *221*, 1047–1048.

In the range $\phi = 0.08-0.05$, structures 3 and 4 coexist on electron micrographs. It has been observed that the diameter of the small unilamellar vesicles produced is of the same order as the in-plane undulation wavelength in the oyster shell state, suggesting a peel-off mechanism from the oyster shell state to the spontaneous unilamellar vesicles.

The question is whether it is general that unbinding occurs as a progressive formation of nearly unilamellar vesicles from the oyster shell state or if the first vesicles formed have an average number of layers of the order of 5–10. This number is given by the ratio of length to in-plane correlation in the undulation instability. Our results point toward the first route in the case of highly charged bilayers where the Debye screening length is larger than the periodicity.

Finally, the answers to the questions raised previously are as follows:

The maximum swelling of the soft lamellar phase with one structural charge per 70 Å occurs around 700 Å.³⁷

A broadening of quasi-Bragg peaks, with the appearance of a superstructure peak due to the periodicity of in-plane

correlations, occurs while giant fluctuations (lateral displacement larger than periodicity) appear for volume fractions between $\phi = 0.11$ and $\phi = 0.05$. This corresponds to the intermediate oyster shell state.

Correlations extend to more than one neighbor, so that first-neighbor-only, undulation as a perturbation, mean field, or Caillé type approaches are no longer valid to interpret Bragg peak shapes.¹² Predictive theories of charged membrane stacking compatible with structure factors as shown in Figure 4 seem to us a challenge for theory of charged membranes since the decrease of scattering seen in SANS for dilute samples is the two-dimensional equivalent of the correlation hole known in the case of polyelectrolytes.

The equation of state of the system determined by complementary scattering experiments under controlled osmotic pressure on either bulk samples or oriented films is given in the second part of this paper.

Acknowledgment. The authors are grateful to J.-C. Dedieu for the freeze-fracture EM experiments and to S. Tristram-Nagle for critical reading of the manuscript.

(37) Rand, R. P.; Parsegian, V. A. *Biochim. Biophys. Acta* **1989**, *988*, 351–376.